Metallophysics and Advanced Technologies
Металофіз. новітні технол.
Metallofiz. Noveishie Tekhnol.
2026, vol. 48, No. 6, pp. 655–667
https://doi.org/10.15407/mfint.48.06.0655
Reprints available directly from the publisher

PACS numbers: 05.70.Ce, 61.43.Dq, 62.20.Qp, 62.80. +f, 64.70.pe, 81.40.Ef, 81.70.Bt

The Effect of Ultrasonic Treatment on the Thermal Stability and Micromechanical Properties of the Amorphous $Co_{67}Fe_3Cr_3Si_{15}B_{12}$ Alloy

T. Tsaregradska, I. Ovsiienko, A. Kuryliuk, I. Plyushchay, V. Kozachenko, G. Saenko, and O. Turkov

Taras Shevchenko National University of Kyiv,
60, Volodymyrs'ka Str.,
UA-01033 Kyiv, Ukraine

The processes of phase formation in an amorphous cobalt-based $Co_{67}Fe_3Cr_3Si_{15}B_{12}$ alloy under the influence of ultrasonic treatment are investigated. The amorphous alloy is obtained by the method of quenching from the melt with a cooling rate of 10^6 K/s in the form of a tape with a thickness of 25 μm and a width of 20 mm. Ultrasonic treatment of samples is carried out in an ultrasonic bath with a maximum ultrasound power of 120 W at a frequency of 44 kHz that allows creating an ultrasound load of 32 W/cm^2. The microhardness of the amorphous alloy is determined by the Vickers method. The characteristics of the thermal stability of amorphous alloys such as the temperature of the beginning of intensive crystallization, as well as the temperature of complete crystallization and the crystallization interval, are studied using highly sensitive dilatometric technique. The structure of the amorphous alloy is also analysed using electron microscopy. As found, ultrasonic treatment of the initial alloy leads to strengthening of the amorphous alloy, as evidenced by an increase in microhardness by 33%. Under the influence of ultrasonic treatment, the temperature interval of thermal stability of the initial alloy decreases, the temperature of the onset of intensive crystallization decreases by 10–85 K depending on the time of ultrasonic

Corresponding author: Iryna Volodymyrivna Ovsiienko
E-mail: irvriaovsiienko@knu.ua

Citation: T. Tsaregradskaya, I. Ovsiienko, A. Kuryliuk, I. Plyushchay, V. Kozachenko, G. Saenko, and O. Turkov, The Effect of Ultrasonic Treatment on the Thermal Stability and Micromechanical Properties of the Amorphous $Co_{67}Fe_3Cr_3Si_{15}B_{12}$ Alloy, *Metallofiz. Noveishie Tekhnol.*, **48**, No. 6: 655–667 (2026). DOI: 10.15407/mfint.48.06.0655

treatment. The obtained results indicate the formation of an amorphous–crystalline state in the initial amorphous $Co_{67}Fe_3Cr_3Si_{15}B_{12}$ alloy under the influence of ultrasonic treatment, which is explained by the creation of thermodynamic conditions for the growth of frozen-in crystallization centres.

Key words: amorphous alloy, ultrasonic treatment, nanocrystalline state, thermal stability, microhardness.

В роботі досліджено процеси фазоутворення в аморфному стопі на основі кобальту $Co_{67}Fe_3Cr_3Si_{15}B_{12}$ за дії ультразвукового оброблення. Вихідний аморфний стоп було одержано методою гартування з розтопу зі швидкістю охолодження у 10^6 К/с у вигляді стрічки товщиною у 25 мкм і шириною у 20 мм. Оброблення аморфного стопу ультразвуком проводили в ультразвуковій ванні з максимальною потужністю у 120 Вт на частоті у 44 кГц, що дало змогу створити ультразвукове навантаження у 32 Вт/см^2. Мікротвердість стопу вимірювали за методою Віккерса. Характеристики термостабільности аморфного стопу досліджували за допомогою високочутливої дилатометричної методики. Структуру аморфного стопу також аналізували за допомогою електронної мікроскопії. Виявлено, що ультразвукове оброблення вихідного стопу приводить до зміцнення аморфного стопу, про що свідчить збільшення мікротвердости на 33%. Під дією ультразвукового оброблення зменшується температурний інтервал термічної стабільности вихідного стопу, температура початку інтенсивної кристалізації зменшується на 10–85 К в залежності від часу ультразвукового оброблення. Одержані результати вказують на формування у вихідному аморфному стопі $Co_{67}Fe_3Cr_3Si_{15}B_{12}$ аморфно-кристалічного стану під впливом ультразвукового оброблення, що пояснено створенням термодинамічних умов для росту вморожених центрів кристалізації.

Ключові слова: аморфний стоп, ультразвукове оброблення, нанокристалічний стан, термічна стабільність, мікротвердість.

(Received 12 November, 2025; in final version, 3 February, 2026)

1. INTRODUCTION

Due to their wide range of applications in many industries, including the military, aerospace, biomedicine and microelectronics, multicomponent amorphous alloys based on cobalt are promising functional materials. Researchers are attracted to amorphous alloys due to their unique chemical and physical properties, such as high fatigue strength, crack resistance, and corrosion resistance. Additionally, these alloys are soft magnetic materials with almost zero magnetostriction [1–3]. However, the widespread use of amorphous alloys is significantly limited by their low thermal stability. When heated to a certain temperature, amorphous metal alloys transform into a more stable crystalline state and lose their unique amorphous properties.

Therefore, one of the directions of research on amorphous alloys is to establish the influence of external factors, such as thermal annealing, radioactive irradiation, mechanical loads, external magnetic and electric fields, on the thermal stability of alloys in the amorphous state. Another important task is to study the thermodynamic conditions for the transition of a metal alloy from an amorphous state to an amorphous-nanocrystalline state. This transition would give the metal alloy new, unique properties due to the interaction between the amorphous matrix and the nanocrystalline structures. These two tasks are often combined into one. At the first stage of crystallisation, a large number of nanocrystalline structures appear in the amorphous matrix. Therefore, it is necessary to establish the thermodynamic prerequisites under which the volume of these nanocrystalline nuclei will not increase. This ensures that the alloy remains in a stable amorphous-nanocrystalline state [4].

One method of converting an amorphous alloy into an amorphous-nanocrystalline state is to process mechanically the alloy, causing intense plastic deformation [5, 6]. Intense plastic deformation of an amorphous alloy can produce a nanocrystalline structure, even when this is not possible using traditional methods such as thermal annealing [7]. The formation of nanosize crystals under shear deformation was first discovered in the amorphous $Fe_{81}Si_7B_{12}$ alloy by the authors in the work [8]. In Ref. [9], it is shown that nanocrystals with sizes up to 15 nm are formed under the action of deformation shear in the amorphous alloy $Fe_{80}B_{20}$, and the number of crystals formed is directly proportional to the degree of deformation. Deformational crystallisation under shear at pressure has also been observed in amorphous ribbons based on aluminium [10–12], titanium and zirconium [13, 14]. Similar processes of nanocrystalline-state formation were observed in amorphous alloys based on iron [15–17], molybdenum [18, 19], nickel [20], with zirconium and niobium [21] during their processing in a high-energy ball mill.

One of the effective methods of mechanical action on amorphous alloys is to subject them to powerful ultrasonic waves. Ultrasonic treatment of amorphous alloys is a more technological and controlled process compared to treatment in high-energy ball mills or in a Bridgman chamber to create shear deformation [22–24]. Studies have shown that powerful ultrasound creates internal compressive stresses, contributing to the formation of a stable nanocrystalline state in an amorphous metal. As found in the work [25], ultrasonic treatment causes structural changes in the amorphous alloy $Fe_{73.6}Si_{15.8}B_{7.2}Cu_{1.0}Nb_{2.4}$ due to the formation of uniformly distributed nanocrystals.

The aim of presented research is to determine the effect of sonication on the thermal stability and micromechanical properties of amorphous $Co_{67}Fe_3Cr_3Si_{15}B_{12}$ alloy.

2. EXPERIMENTAL DETAILS

The multicomponent amorphous $Co_{67}Fe_3Cr_3Si_{15}B_{12}$ alloy has been chosen for studying of crystallization process under ultra sonic treatment. The amorphous alloy has been obtained by the method of quenching from the melt with a cooling rate of 10^6 K/s in the form of a tape with a thickness of 25 μm and a width of 20 mm. To ensure relaxation of mechanical stresses existing in amorphous alloys obtained by the spinning method, the studied samples were previously aged under normal conditions for 5 years.

Ultrasonic treatment of samples was carried out in an ultrasonic bath with a maximum ultrasound power of 120 W at a frequency of 44 kHz, which allowed creating an ultrasound load of 32 W/cm^2. The ultrasonic bath was filled with distilled water, after which samples of the amorphous alloy were placed in it. The samples were kept under ultrasonic loading for a certain time, after which they were removed from the bath. Ultrasonic treatment of amorphous alloys was carried out at room temperature, which is significantly lower than the relaxation temperature of amorphous alloys.

The microhardness of the amorphous alloy was determined by the Vickers method: a diamond pyramid with a load of 50 g was pressed into the material under study and the diagonal of the resulting imprint was measured. Microhardness H_V was defined as

$$H_V = \frac{1854P}{d^2} \text{ N/mm}^2, \tag{1}$$

where P is a load in newtons, d is the length of the diagonal of the imprint in millimetres.

Microhardness measurements were made in air at room temperature. The indenter was pressed on the shiny side of the amorphous ribbon, which was not in contact with the rotating drum during its acquisition. The microhardness measurement error did not exceed 5%.

The characteristics of the thermal stability of amorphous alloys such as the temperature of the beginning of intensive crystallization, as well as the temperature of complete crystallization and the crystallization interval has been studied using highly sensitive dilatometric technique [26]. The dilatometric method is based on the fact that the molar volumes of alloys differ between their amorphous and crystalline states. The difference in molar volume between the amorphous and crystalline states is 1–3%. Measurements of the samples' length were performed within a temperature range of 290–940 K. The samples of source amorphous alloy and amorphous alloy after ultrasonic treatment were heated at a constant speed of 10 K/min. The length of the samples was measured every 5 K.

3. RESULTS AND DISCUSSION

3.1. Effect of Ultrasonic Treatment on the Microhardness of Amorphous $Co_{67}Fe_3Cr_3Si_{15}B_{12}$ Alloy

Microhardness studies were conducted on the initial amorphous $Co_{67}Fe_3Cr_3Si_{15}B_{12}$ alloy and the same alloy subjected to ultrasonic treatment at a frequency of 44 kHz and a power of 32 W/cm^2, to establish the effect of ultrasonic treatment.

The microhardness values, as well as the relative change in the microhardness of the amorphous alloy sample after ultrasonic treatment depending on the treatment time, are given in Table 1. The time dependence of the relative change in the microhardness of the amorphous alloy is also given in Fig. 1.

As can be seen in Fig. 1 and Table 1, changes in microhardness do not exceed the measurement error (*i.e.*, 5%), if the ultrasonic treatment time does not exceed 90 s. As the ultrasonic treatment time increases, the microhardness also increases. At treatment times of up to 1500 s, the relative increase in microhardness is more than 30%. However, if the treatment time exceeds 1500 s, the increase in microhardness is inhibited and it reaches saturation.

Let us analyse the physical reasons for the change in microhardness under the influence of ultrasonic treatment. Microhardness, as well as other micromechanical properties of amorphous alloys, depends on the chemical composition of the amorphous matrix, the presence of frozen crystallization centres in it, and internal mechanical stresses. Microhardness of amorphous alloys increases significantly when crystalline phases form in amorphous alloys. This effect is especially noticeable in the presence of borides and silicides in the structure of the amorphous

TABLE 1. Microhardness H_V and relative change in the microhardness $(H_V - H_{V0})/H_{V0}$ of the amorphous alloy sample after ultrasonic treatment depending on the treatment time t.

Ultrasonic treatment time t, s	H_V, Pa	$(H_V - H_{V0})/H_{V0}$, %
Source sample	727	–
90	745	2.5
180	782	7.6
280	794	9.0
480	818	12.5
1440	950	31.0
2880	960	32.0
3360	966	33.0

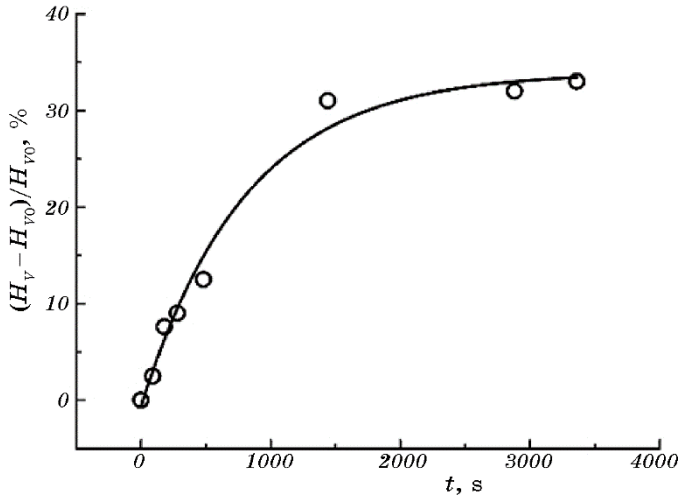

Fig. 1. The time dependence of the relative change in the microhardness of the amorphous $Co_{67}Fe_3Cr_3Si_{15}B_{12}$ alloy.

alloy. In general, the hardness of the nanostructured state is higher than that of an amorphous similar composition.

Ultrasonic treatment of amorphous alloy leads to an increase in the diffusion mobility of atoms and enhances the phenomenon of internal friction. In addition, ultrasound causes internal heating of the amorphous alloy due to the absorption of energy in the process of internal friction, which also stimulates the acceleration of diffusion. These processes accelerate the structural relaxation of the amorphous alloy and stimulate its nanocrystallization, which occurs due to atomic displacements during intense plastic deformation.

3.2. Effect of Ultrasonic Treatment on the Thermal Stability of Amorphous $Co_{67}Fe_3Cr_3Si_{15}B_{12}$ Alloy

Figure 2 shows the experimentally obtained temperature dependences of the relative change in molar volume for the initial amorphous alloy and for the amorphous alloy after ultrasonic treatment at a frequency of 44 kHz at a power of 32 W/cm^2 for 3360 s.

As can be seen in Fig. 2, ultrasonic treatment of the initial $Co_{67}Fe_3Cr_3Si_{15}B_{12}$ alloy for 3360 s leads to a significant (by 85 K) shift of the temperature of the onset of intensive crystallization towards low temperatures. At the same time, the temperature interval, in which complete crystallization of the ultrasonically treated amorphous alloy occurs, expands to 75 K compared to the initial amorphous $Co_{67}Fe_3Cr_3Si_{15}B_{12}$ alloy, for which this interval is of 65 K. Similar tem-

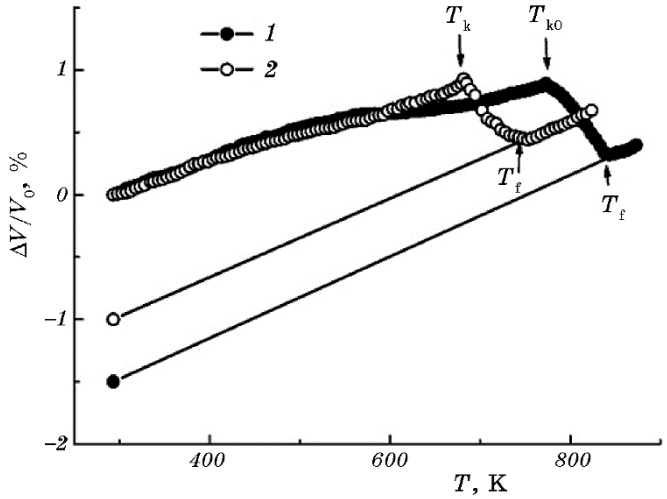

Fig. 2. The temperature dependence of the relative change in molar volume for the initial (*1*) and subjected to ultrasonic treatment for 3360 s (*2*) amorphous $Co_{67}Fe_3Cr_3Si_{15}B_{12}$ alloy.

TABLE 2. Thermal stability parameters of the source and ultrasonically treated amorphous $Co_{67}Fe_3Cr_3Si_{15}B_{12}$ alloy: ultrasonic treatment time t, temperature of onset (T_k) and complete (T_f) of crystallization, interval ΔT_k, by which the temperature of the onset of intensive crystallization decreases, and interval of full crystallization ΔT_{cr} after ultrasonic treatment ΔT_k.

t, s	T_k, K	$\Delta T_k = T_k - T_{k0}$, K	T_f, K	$\Delta T_{cr} = T_f - T_k$, K
Source alloy	$T_{k0} = 773$	–	838	65
180	773	0	847	74
280	768	−5	843	75
480	753	−20	833	80
1440	723	−50	813	90
2880	703	−70	798	95
3360	680	−85	755	75

perature dependences of the relative change in volume were obtained for the amorphous $Co_{67}Fe_3Cr_3Si_{15}B_{12}$ alloy after ultrasonic treatment within the interval from 180 s to 2880 s. The measurement results are given in Table 2.

As can be seen from Table 2, short ultrasonic treatment times do not affect the temperature at which intensive crystallisation begins (temperature changes are within the margin of error). However, increasing the ultrasonic treatment time causes a decrease in the temperature, at

which intensive crystallisation begins.

Figure 3 presents the dependence of the temperature interval $\Delta T_k = T_k - T_{k0}$, by which the temperature of the onset of intensive crystallization for amorphous $Co_{67}Fe_3Cr_3Si_{15}B_{12}$ alloy decreases, on the time of ultrasonic treatment.

As can be seen in Fig. 3, the dependence of the temperature interval ΔT_k, by which the temperature of the onset of intensive crystallization of amorphous $Co_{67}Fe_3Cr_3Si_{15}B_{12}$ alloy decreases, on the ultrasonic treatment time is close to being linearly. In addition, as can be seen in Table 2, the temperature interval at which the amorphous alloy completely crystallises increases slightly with increasing ultrasonic treatment time.

Let us analyse the obtained results. As well known, the highest frequency of crystalline phase nucleation during the rapid cooling of a melt occurs, when its temperature reaches $0.7T_m$. At this temperature, the heterogeneous system 'amorphous matrix–frozen crystallisation centres' is formed. However, for an alloy to be considered amorphous, the crystalline phase fraction in the system should not exceed 10^{-6}. The system 'amorphous matrix–frozen crystallisation centres' is in thermodynamic equilibrium, when the difference in chemical potentials of the i-th phase in the liquid ($\Delta\mu_{i0}^{\alpha}$) and crystalline ($\Delta\mu_{i0}^{\beta}$) states is zero:

$$\Delta\mu_{i0}^{\alpha-\beta} = \Delta\mu_{i0}^{\alpha} - \Delta\mu_{i0}^{\beta} = 0. \qquad (2)$$

In the system 'amorphous matrix–frozen crystallization centres'

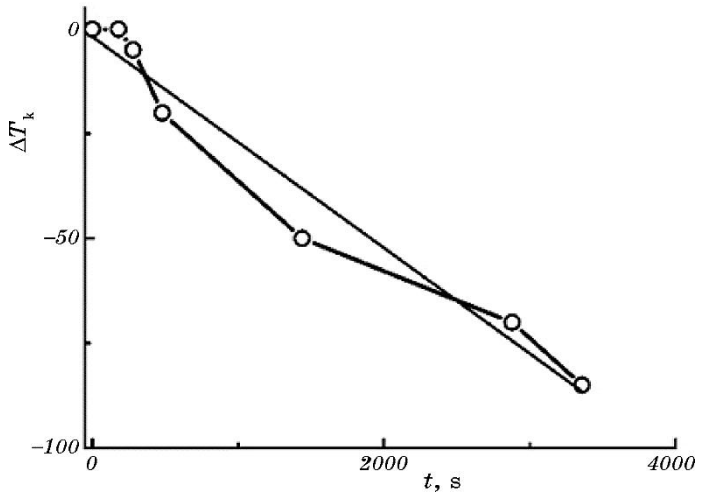

Fig. 3. The dependence of the temperature interval $\Delta T_k = T_k - T_{k0}$, by which the temperature of the onset of intensive crystallization of amorphous $Co_{67}Fe_3Cr_3Si_{15}B_{12}$ alloy decreases, on the time of ultrasonic treatment.

elastic stresses are always present due to the difference in volume between the amorphous and crystalline phases. Ultrasonic treatment of an amorphous alloy results in additional elastic deformations occurring at the interface between the crystalline and amorphous phases. These deformations lead to reduction of the difference in chemical potentials of the i-th component $\Delta\mu_i^{\alpha-\beta}$ in the liquid and crystalline phases, compared to a state without elastic deformations:

$$\Delta\mu_i^{\alpha-\beta} = -(P_\beta V_\beta - P_\alpha V_\alpha) + \Delta\mu_{i0}^{\alpha-\beta}, \quad (3)$$

where $P_{\alpha,\beta}$ is the respective pressure in α- and β-phases at the α–β interface, and $V_{\alpha,\beta}$ is the respective molar volume of α- and β-phases.

In the work [27], an expression for the difference in chemical potentials of the i-th component in the α- and β-phases has been obtained in the spherical crystal nucleus approximation, taking into account the influence of elastic deformations on the interface of the α- and β-phases:

$$\Delta\mu_i^{\alpha-\beta} = -\frac{\chi_T^\alpha V_\beta + \chi_T^\beta V_\alpha}{\chi_T^\alpha + \chi_T^\beta}\frac{2\sigma}{r_{0P}} - \frac{(V_\beta - V_\alpha)(\bar{V}_i^\beta - \bar{V}_i^\alpha)}{(\chi_T^\alpha + \chi_T^\beta)\bar{V}}\left[1 - \left(\frac{r_0}{r_{0P}}\right)^3\right] + \Delta\mu_{i0}^{\alpha-\beta}(T), \quad (4)$$

$$\Delta\mu_{i0}^{\alpha-\beta} = \frac{\Delta H_{0i}(T_{Pi} - T)}{T} + RT\ln\frac{\alpha_i^\alpha(C_i^\alpha, T)}{\alpha_i^\beta(C_i^\beta, T)},$$

where χ_T^α and χ_T^β are the isothermal compressibility coefficients, and $\bar{V}_i^\alpha$, $\bar{V}_i^\beta$ are the partial molar volumes for the α- and β-phases, respectively, α_i^α and α_i^β are the activities, and C_i^α, C_i^β are the concentrations of i-th component for the α- and β-phases, respectively, σ is the specific surface energy, r_0 and r_{0P} are the radii of spherical crystal nuclei in the absence of pressure at the interface between the liquid and crystal phases and in presence of it, ΔH_{0i} and T_{Pi} are the enthalpy of fusion and the melting point, respectively, of the i-th component.

These equations were used to construct the dependence of the difference in chemical potentials of the i-th component in the liquid and crystalline phases on the supercooling value, which is shown in Fig. 4 [27].

As well known, the difference in chemical potentials of the i-th component in the amorphous and crystalline states decreases monotonically with increasing temperature. As mentioned above, at $T = 0.7T_m$, it becomes zero, representing thermodynamic equilibrium in the 'amorphous matrix–frozen-in crystallisation centres' system. However, in the temperature range below the temperature $0.7T_m$, the dependence $\Delta\mu(T)$ deviates from monotonic type. In this range, local minima and maxima in dependence $\Delta\mu(T)$ as well as a change in sign of $\Delta\mu$ are observed.

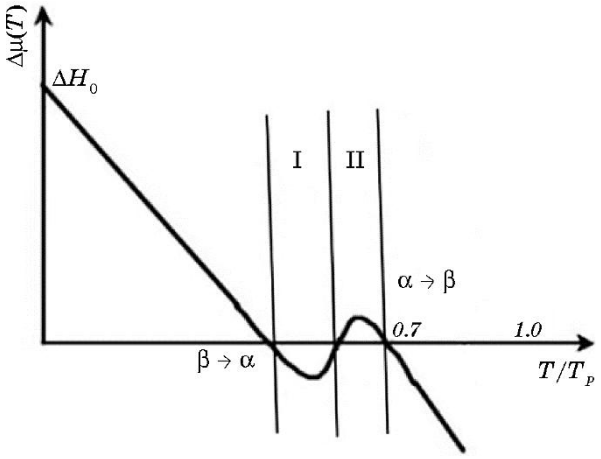

Fig. 4. The calculated dependence of the difference in chemical potentials of the *i*-th component in the liquid and crystalline phases on the supercooling value [27].

Let us take a closer look at these temperature ranges. In temperature interval I, the dissolution of nuclei of the crystalline phase that have already formed occurs due to the process of upward diffusion, which is caused by the difference in the chemical potential of the *i*-th component in the amorphous and crystalline phases [28]. In temperature region II, where $\Delta\mu$ is positive, frozen crystallisation centres form without their volume growing any further. Note that this complex form of temperature dependence chemical potential difference is caused by significant mechanical stresses in the amorphous matrix resulting from the different molar volumes of the *i*-th component in the liquid and crystalline phases, which are enhanced by ultrasonic treatment of the alloy.

Ultrasonic treatment of the initial alloy for a significant time causes local heating and an increase in the alloy's temperature. As a result, the 'amorphous matrix–frozen-in crystallisation centres' system transitions from temperature interval I, where dissolution of the crystalline phase nuclei occurs due to upward diffusion ($\Delta\mu(T) < 0$), to temperature region II ($\Delta\mu(T) < 0$), in which a significant number of nanosize crystalline phase nuclei form without increasing in size.

This conclusion is confirmed by data from electron-microscopy studies of the structure of the source and ultrasonically treated alloys (Fig. 5).

As can be seen in Fig. 5, before ultrasonic treatment, there are a few large crystal nuclei in the amorphous matrix. After ultrasonic treatment, a significant number of small crystallisation centres appear and are distributed evenly throughout the matrix. The formation of a

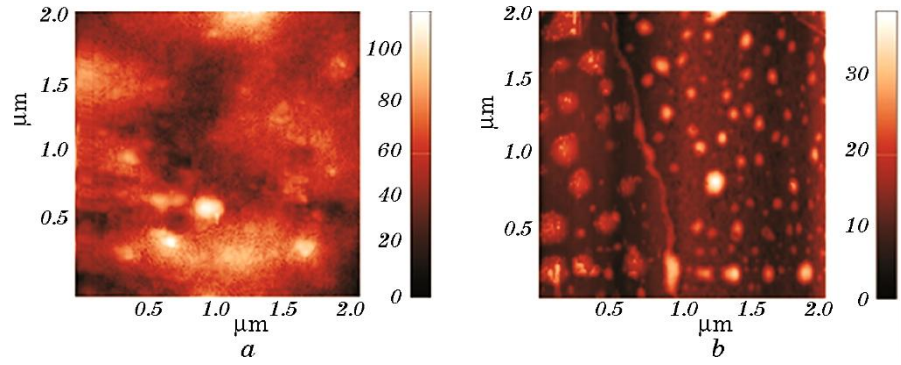

Fig. 5. Electron-microscopy images of the $Co_{67}Fe_3Cr_3Si_{15}B_{12}$ alloy before (*a*) and after (*b*) ultrasonic treatment.

large number of nanosize crystals following the ultrasonic treatment of an amorphous alloy is responsible for the increase in microhardness of treated alloy. Therefore, ultrasonic treatment of an amorphous alloy can be considered as a method of obtaining an amorphous-nanocrystalline state due to the controlled growth of frozen-in crystallization centres in an amorphous alloy.

4. CONCLUSION

Experimental studies have shown that ultrasonic treatment leads to changes in the micromechanical properties and thermal stability parameters of an amorphous alloy. Experimental studies have shown that ultrasonic treatment leads to changes in the micromechanical properties and thermal stability parameters of an amorphous $Co_{67}Fe_3Cr_3Si_{15}B_{12}$ alloy. Ultrasonic treatment strengthens the amorphous alloy as evidenced by an increase in its Vickers microhardness between 8% and 33%, depending on the treatment time.

The thermal stability of the amorphous alloy decreases under the influence of ultrasonic treatment. The temperature at which intensive crystallization begins decreases by 0.6–11% depending on the treatment time, while the temperature range at which complete crystallization of the amorphous alloy occurs slightly increases with increasing ultrasonic treatment time.

In addition, it has been experimentally established that temperature interval ΔT_k, by which the temperature of the onset of intensive crystallization of amorphous $Co_{67}Fe_3Cr_3Si_{15}B_{12}$ alloy decreases, is directly proportional to the time of ultrasonic treatment of the source alloy.

Electron-microscopy studies of the structure of the original and ultrasonically treated amorphous alloy confirm the formation of an amorphous–nanocrystalline state in the alloy as a result of ultrasonic

treatment.

So, ultrasonic treatment creates the thermodynamic conditions necessary for a controlled increase in the number of frozen crystallisation centres in the amorphous matrix and, consequently, for the alloy, to transition from amorphous state to amorphous–nanocrystalline one.

AUTHORS' CONTRIBUTIONS

T. Tsaregradska: conceptualization, data curation, formal analysis, writing original draft. I. Ovsiienko: literature review, writing original draft, review and editing. A. Kuryliuk: investigation, formal analysis. I. Plyushchay: formal analysis, validation. V. Kozachenko: investigation. G. Saenko: investigation, formal analysis. O. Turkov: investigation. All authors approved the final version of the manuscript.

REFERENCES

1. H. Jiang, T. Shang, H. Xian, B. Sun, Q. Zhang, Q. Yu, H. Bai, L. Gu, and W. Wang, *Small Structures*, **2**, Iss. 2: 2000057 (2021).
2. Z. Feng, H. Geng, Yu. Zhuang, and P. Li, *Inorganics*, **12**, Iss. 9: 232 (2024).
3. P. Rani, V. Kurichenko, E. Gürbüz, B. Sanyal, B. Hjörvarsson, and G. Andersson, *Phys. Rev. B*, **108**: 134412 (2023).
4. F. C. Li, T. Liu, J. Y. Zhang, S. Shuang, Q. Wang, A. D. Wang, J. G. Wang, and Y. Yang, *Mater. Today Advances*, **4**: 100027 (2019).
5. S. Chen, J. Wang, L. Xia, and Yu. Wu, *Entropy*, **21**, Iss. 1: 54 (2019).
6. K. Csach, J. Miškuf, and A. Jurıková, *J. Phys.: Conf. Ser.*, **200**: 082002 (2010).
7. H. J. Jin, F. Zhou, L. B. Wang, and K. Lu, *Scripta Mater.*, **44**, Iss. 7: 1083 (2001).
8. M. O. Vasylyev, V. K. Nosenko, I. V. Zagorulko, and S. M. Voloshko, *Progress in Physics of Metals*, **21**, No. 3: 319 (2020).
9. G. E. Abrosimova, A. S. Aronin, S. V. Dobatkin, I. I. Zver'kova, D. V. Matveev, and O. G. Rybchenko, *Phys. Metals Metallography*, **106**: 597 (2008).
10. Zs. Kovács, P. Henits, A. P. Zhilyaev, and A. Révész, *Scripta Mater.*, **54**, Iss. 10: 1733 (2006).
11. N. Boucharat, R. Hebert, H. Rösner, R. Valiev, and G. Wilde, *Scripta Mater.*, **53**, Iss. 7: 823 (2005).
12. N. Boucharat, R. J. Hebert, H. Rösner, and G. Wilde, *Solid State Phenomena*, **114**: 123 (2006).
13. M. Tao, A. Chokshi, R. Conner, G. Ravichandran, and W. Johnson, *J. Mater. Research*, **25**: 1137 (2010).
14. D. Stryż, J. Palka, Z. Lekston, and G. Dercz, *Mater. Sci. Forum*, **738–739**: 501 (2013).
15. C. Zhang, Z. Zhang, Z. Qi, Y. Qi, J. Zhang, and X. Bian, *J. Non-Cryst. Solids*, **354**, Iss. 32: 3812 (2008).
16. T. Gheiratmand, H. R. M. Hosseini, P. Davami, G. Ababei, and M. Song, *Metall. Mater. Trans. A*, **46**: 2718 (2015).
17. J.-J. Kim, Y. Choi, S. Suresh, and A. S. Argon, *Science*, **295**, No. 5555: 654

(2002).
18. F. Q. Guo and K. Lu, *Metall. Mater. Trans. A*, **28**: 1123 (1997).
19. B. Yao, S.-E. Liu, L. Liu, L. Si, W.-H. Su, and Y. Li. *J. Appl. Phys.*, **90**: 1650 (2001).
20. G. J. Fan, M. X. Quan, Z. Q. Hu, W. Löser, and J. Eckert. *J. Mater. Research*, **14**: 3765 (1999).
21. M. L. Trudeau, R. Schulz, D. Dussault, and A. Van Neste, *Phys. Rev. Lett.*, **64**: 99 (1990).
22. B. N. Mordyuk and G. I. Prokopenko. *J. Sound Vibration*, **308**, Iss. 3–5: 855 (2007).
23. H. Chen, Y. He, G. J. Shiflet, and S. J. Poon, *Nature*, **367**: 541 (1994).
24. W. H. Jiang and M. Atzmon, *Acta Mater.*, **51**, Iss. 14: 4095 (2003).
25. M. A. Vasilev, V. A. Tinkov, Ju. N. Petrov, S. M. Voloshko, G. G. Galstjan, V. T. Cherepin, and A. S. Khodakovskij, *Metallofiz. Noveishie Tekhnol.*, **35**, No. 5: 667 (2013) (in Russian).
26. V. I. Lysov, T. L. Tsaregradskaya, O. V. Turkov, and G. V. Saenko, *J. Phys. Studies*, **15**: 2704 (2011).
27. V. I. Lysov, T. L. Tsaregradskaya, A. M. Kurylyuk, O. V. Turkov, and G. V. Saenko, *J. Phys. Studies*, **22**: 3702 (2018) (in Ukrainian).
28. V. I. Lysov, T. L. Tsaregradskaya, G. V. Saenko, and O. V. Turkov, *Bull. Kyiv Nat. Univ. Phys. Math. Sci.*, No. 2: 259 (2015) (in Ukrainian).